Published in final edited form as:
Eur J Neurosci. 2006 June ; 23(11): 2983–2990.

Calcium-induced calcium release in rod photoreceptor terminals boosts synaptic transmission during maintained depolarization

Lucia Cadetti[1], **Eric J. Bryson**[1], **Cory A. Ciccone**[1], **Katalin Rabl**[1], and **Wallace B. Thoreson**[1,2]

1 *Department of Ophthalmology & Visual Science, University of Nebraska Medical Center, Omaha, NE 68198-5840, USA*

2 *Department of Pharmacology & Experimental Neuroscience, University of Nebraska Medical Center, Omaha, NE 68198-5840, USA*

Abstract

We examined the contribution of calcium-induced calcium release (CICR) to synaptic transmission from rod photoreceptor terminals. Whole-cell recording and confocal calcium imaging experiments were conducted on rods with intact synaptic terminals in a retinal slice preparation from salamander. Low concentrations of ryanodine stimulated calcium increases in rod terminals, consistent with the presence of ryanodine receptors. Application of strong depolarizing steps (−70 to −10 mV) exceeding 200 ms or longer in duration evoked a wave of calcium that spread across the synaptic terminals of voltage-clamped rods. This secondary calcium increase was blocked by high concentrations of ryanodine, indicating it was due to CICR. Ryanodine (50 μM) had no significant effect on rod calcium current (I_{ca}) although it slightly diminished rod light-evoked voltage responses. Bath application of 50 μM ryanodine strongly inhibited light-evoked currents in horizontal cells. Whether applied extracellularly or delivered into the rod cell through the patch pipette, ryanodine (50 μM) also inhibited excitatory post-synaptic currents (EPSCs) evoked in horizontal cells by depolarizing steps applied to rods. Ryanodine caused a preferential reduction in the later portions of EPSCs evoked by depolarizing steps of 200 ms or longer. These results indicate that CICR enhances calcium increases in rod terminals evoked by sustained depolarization, which in turn acts to boost synaptic exocytosis from rods.

Keywords

bipolar cell; calcium stores; horizontal cell; retina; ryanodine; salamander

Introduction

Photoreceptors are tonically depolarized in darkness, permitting a continuous influx of calcium through L-type calcium channels that stimulates continuous release of the neurotransmitter, glutamate. Calcium influx can also trigger a calcium-induced release of calcium from endoplasmic reticulum that appears to contribute to synaptic release from rods (Krizaj *et al*., 1999, 2003; Suryanarayanan & Slaughter, 2006). The regulation of intracellular calcium levels by these mechanisms is essential for accurately encoding visual information at the photoreceptor synapse, but maintenance of proper calcium levels is also important for maintaining the viability of photoreceptors and avoiding excitotoxic damage to downstream neurons that can be produced by excessive glutamate release (Crosson *et al*., 1990; Edward *et*

Correspondence: Dr W. B. Thoreson, [1]Department of Ophthalmology, as above. E-mail: wbthores@unmc.edu.

al., 1991; Fox *et al*., 2003; Sharma & Rohrer, 2004; Doonan *et al*., 2005; Hemara-Wahanui *et al*., 2005). To understand better the regulation of intracellular calcium levels in rod photoreceptors, we examined the kinetics of the relationship between calcium influx and calcium-induced calcium release (CICR) in rod terminals and tested the contribution of CICR to synaptic release.

Smooth endoplasmic reticulum is present in the inner segments and synaptic terminals of photoreceptors (Mercurio & Holtzman, 1982) where it accumulates calcium ions (Ungar *et al*., 1981). Immunohistochemical studies suggest the presence of Type II ryanodine receptors, which mediate CICR from endoplasmic reticulum, in the synaptic terminals of rods and cones in the salamander retina (Krizaj *et al*., 2003, 2004). Furthermore, calcium imaging studies on isolated rods showed caffeine-evoked calcium increases in rod terminals and inner segments that were blocked by ryanodine, suggesting an action at ryanodine receptors (Krizaj *et al*., 1999). The caffeine-evoked calcium increases in rod cells were followed by a depression of intracellular calcium. Therefore, the finding that caffeine decreased glutamate release from a photoreceptor sheet preparation and hyper-polarized the resting membrane potential of second-order retinal horizontal cells is consistent with a role for CICR in synaptic transmission from rods (Krizaj *et al*., 1999). However, interpretation of these experiments is confounded by the actions of caffeine at other sites including calcium currents (I_{Ca}) in rods (Krizaj *et al*., 1999), phosphodiesterase activity (Smith & Mills, 1970), IP3 receptors (Collin *et al*., 2005), adenosine receptors (Boulenger *et al*., 1982) and horizontal cells (Linn & Gafka, 2001; Hayashida & Yagi, 2002). To avoid these complications, we examined the contribution of CICR to synaptic transmission from photoreceptors by using ryanodine, which is more highly selective for the ryanodine receptor than caffeine. Unlike for caffeine, we found that ryanodine had no significant effect on photoreceptor I_{Ca}. Ryanodine also has the useful property of acting as an agonist to stimulate release of calcium from intracellular stores at low concentrations (≤ 1 μM) but acting as an antagonist to block CICR at high concentrations (Rousseau *et al*., 1987; Pessah & Zimanyi, 1991). Based on the effects of ryanodine on synaptic transmission, Suryanarayanan & Slaughter (2006) recently suggested that CICR amplifies release from rods. We used confocal calcium imaging to study the effects of ryanodine on CICR and simultaneous paired recordings from photoreceptors and post-synaptic neurons in a retinal slice preparation to study its effects on synaptic transmission.

The results showed the presence of ryanodine-sensitive calcium changes in synaptic terminals of rods in the retinal slice with a prominent contribution from CICR to intraterminal calcium levels evoked by depolarizing voltage steps maintained for 200 ms or longer. Consistent with effects on intraterminal calcium levels, blocking CICR with ryanodine preferentially reduced later portions of horizontal cell excitatory post-synaptic currents (EPSCs) evoked by steps of 200 ms or longer applied to rods. The results indicate that CICR boosts synaptic transmission from rod photoreceptors during maintained depolarization.

Materials and methods

Preparations

Experiments were performed using retinas from the aquatic tiger salamander (*Ambystoma tigrinum*, 18–25 cm). Care and handling procedures were approved by the UNMC Institutional Animal Care and Use Committee. The salamander was decapitated and the brain and spinal cord were rapidly pithed. After enucleation, the anterior segment of the eye, including the lens, was removed. The resulting eyecup was cut into quarters and a section of eyecup was placed vitreal side down on a piece of filter paper (2 × 5 mm, Type AAWP, 0.8-μm pores, Millipore, Bedford, MA, USA). After adhering to the filter paper, the retina was isolated under cold amphibian Ringer's solution (see composition below). Retinal slices (125 μm) were cut with a razor blade tissue chopper (Stoelting, Wood Dale, IL, USA) and positioned in the recording

chamber to allow viewing of the retinal layers with an upright fixed-stage microscope (Olympus BHWI, Tokyo, Japan or Nikon E600 FN, Japan).

Slices were superfused at ~1 mL/min with an oxygenated amphibian Ringer's solution containing (in mM): 111 NaCl, 2.5 KCl, 1.8 $CaCl_2$, 0.5 $MgCl_2$, 10 HEPES, 5 glucose, 0.1 picrotoxin, 0.001 strychnine (pH 7.8). Osmolarity was tested with a vapor pressure osmometer (Wescor, Logan, UT, USA) and adjusted, if necessary, to ~242 mOsm. Unless otherwise specified, chemicals were obtained from Sigma-Aldrich (St. Louis, MO, USA).

Electrophysiology

Ruptured patch whole-cell recordings were obtained using 8–15 MΩ patch electrodes pulled from borosilicate glass (1.2 mm OD, 0.95 mm ID, with internal filament, World Precision Instruments, Sarasota, FL, USA) on a PP-830 micropipette puller (Narishige USA, East Meadow, NY, USA). The pipette solution contained (in mM): 94 Cs gluconate, 9.4 TEA Cl, 1.9 $MgCl_2$, 9.4 MgATP, 0.5 GTP, 0.5 or 5 EGTA, 32.9 HEPES (pH 7.2). The osmolarity was measured with a vapor pressure osmometer (Wescor) and adjusted, if necessary, to ~242 mOsm.

Ryanodine was a gift from Dr Keshore Bidasee, University of Nebraska Medical Center. It was dissolved in ethanol and diluted ≥ 1 : 1000 into patch pipette or bathing solutions. Solvent controls showed no significant effect of ethanol diluted 1 : 1000 on EPSC waveform or rod light responses. We bath applied ryanodine only once on any retinal slice to avoid potential complications owing to the difficulty of reversing its effect following washout.

Cells were voltage clamped using a Multiclamp (Axon Instruments, Foster City, CA, USA) or Optopatch (Cairn Instruments, Faversham, Kent, UK) patch-clamp amplifier. Recording pipettes were positioned with Huxley-Wall micromanipulators (Sutter Instruments, Novato, CA, USA). Acceptable access resistances for voltage clamp recordings were < 50 MΩ. Currents were acquired using a Digidata 1322 interface and pClamp 8.1 software (Axon Instruments). Photoreceptors were voltage clamped at −70 mV, bipolar cells at −50 mV and horizontal cells near their resting potential (typically −50 or −60 mV). Rods and cones were distinguished morphologically. Horizontal, ON and OFF bipolar cells were distinguished by physiological criteria (Thoreson *et al*., 1997). In many instances, the identities of pre- and post-synaptic cells were confirmed anatomically by use of a fluorescent tracer, Lucifer Yellow (2 mg/mL), added to the pipette solution. Passive cell properties were similar to those reported by Cadetti *et al*. (2005). Under our recording conditions, charging curves for rods, bipolar cells and many horizontal cells can be fit by single exponentials, indicating a compact electrotonic structure. The good single exponential fit to the charging curves of many horizontal cells suggests they were largely uncoupled from their neighbors in the retinal slice preparations used for these studies.

Light stimuli were generated by a tungsten light source and reflected into the microscope condenser pathway using a beam splitter. Light intensity was controlled by neutral density filters (Wratten gel) and wavelength by interference filters. The intensity of unattenuated light measured with a laser power meter (Metrologic) was 1.3×10^6 photons/s/μm^2 at 580 nm. A flash duration of 1 s was generally used.

Imaging

Confocal images were acquired using a laser confocal scanhead (Perkin Elmer Ultraview LCI) equipped with a cooled CCD camera (Orca ER) mounted to a fixed-stage upright microscope (Nikon E600 FN). Images were binned 2 × 2. Images were acquired at 60-ms intervals and each image had a single frame duration of 48–56 ms. Excitation and emission were controlled

by a Sutter Lambda 10-2 filter wheel and controller. Images were acquired and analysed using UltraView Imaging Suite software. The objective (60, 1.0 NA) was controlled using a Z-axis controller (E662 Physik Instrumente, Germany) to visualize either a single confocal slice or a series of slices (1-μm steps).

In some experiments, photoreceptors were loaded with the calcium-sensitive dye Fluo4 (K_d = 345 nM), by incubating retinal slices for 45 min in the dark with 0.5 mL of 10 μM Fluo4-AM + 5 μM pluronic F-127 (Molecular Probes, Eugene, OR, USA), followed by an additional incubation in Fluo4-AM alone for 1.5 h in a slice chamber at 5 °C. In other experiments, the calcium-sensitive dye was added to the patch pipette solution at a concentration of 0.1 mM and loaded directly into the cell during whole-cell recording. For this approach, we used three different dyes: Oregon Green 488 BAPTA-1, which has a K_d of 0.17 μM, as well as its lower affinity isomers Oregon Green 488 BAPTA-6F and Oregon Green 488 BAPTA-5N, which have K_d values of 3 and 20 μM, respectively. For single-wavelength dyes such as Oregon Green and Fluo4, the change in fluorescence relative to baseline fluorescence ($\Delta F/F$) provides a measure of intracellular [Ca^{2+}] independent of changes in dye concentration (Helmchen, 2000).

The criterion for statistical significance was chosen to be $P < 0.05$ and evaluated with Student's *t*-test using GraphPad Prism 4. Variability is reported as ± SEM.

Results

Using a confocal microscope, we examined calcium levels from individual rods and cones in retinal slices loaded with the calcium-sensitive dye Fluo4-AM (Fig. 1). To test for the presence of CICR in photoreceptor terminals, we applied ryanodine at a low concentration (1 μM), at which it acts as an agonist to stimulate release of calcium from intracellular stores (Rousseau *et al*., 1987;Pessah & Zimanyi, 1991). Bath application of 1 μM ryanodine stimulated calcium increases in the terminals, as well as cell bodies, of rod photoreceptor cells. The arrows in Fig. 1 indicate three rod terminals, two of which showed a fluorescence increase in response to ryanodine. The images in this figure show compiled stacks of confocal images obtained at 1-μm intervals, but we also confirmed intraterminal fluorescence increases by examining changes in individual confocal sections. Similar increases in rod calcium levels were observed following bath application of 1 μM ryanodine in seven retinal slices. These results using intact photoreceptors from retinal slices confirm previous studies using isolated photoreceptors, which, because of the difficulty in obtaining isolated cells with intact terminals, were largely limited to inner segment measurements of CICR (Krizaj *et al*., 1999,2003).

To examine the spatiotemporal changes in intraterminal calcium evoked by presynaptic depolarization, we obtained whole-cell recordings from rods and loaded via the patch pipette with a calcium-sensitive fluorescent dye. Cells were stimulated by depolarizing test steps (−70 to −10 mV) of varying duration (50 ms to 1 s). Figure 2 shows examples of fluorescence changes in a single confocal section of a rod terminal loaded with Oregon Green 488 BAPTA-1 (100 μM). The image acquisition time was 55 ms per frame and images were acquired every 60 ms. The figure was cropped to emphasize the synaptic terminal that is attached by a thin axon to the base of the soma. Panel A shows fluorescence levels in the terminal before (Fig. 2A, 1), during (Fig. 2A, 2) and after (Fig. 2A, 3, and A4) a 50-ms depolarizing step. The image in Fig. 2A, 2, shows the calcium increase integrated over the entire 50 ms of the short step. Panel B shows calcium levels in the terminal before (Fig. 2B, 1), during (Fig. 2B, 2 and 3) and after (Fig. 2B, 4) a 500-ms depolarizing step. For both the long and the short test steps, the first image acquired during the step revealed a pair of bright spots, the larger of which is indicated by arrows in the figure (Fig. 2, A2 and B2). The bright spots presumably correspond to clusters of calcium channels, which create strong sites of calcium influx (Nachman-Clewner *et al*.,

1999;Zenisek *et al*., 2004). After termination of the 50-ms step, the terminal calcium change recovered to control levels within 250 ms (Fig. 2A, 3). With the longer step, maintaining the depolarization for an additional 250 ms triggered a secondary spread of fluorescence throughout the terminal (Fig. 2B, 3). This secondary spread of fluorescence through the terminal was consistently evoked by steps of 200 ms or longer ($n = 7$) but never evoked by 50-ms steps. The image in Fig. 2B, 4, shows that calcium levels remained elevated in the terminal 2 s after the end of the 500-ms step.

Experiments illustrated in Fig. 2 were conducted using Oregon Green 488 BAPTA-1, which has a K_d of 0.17 μM. However, calcium levels at sites of calcium influx may exceed this concentration and thus saturate the dye. We therefore repeated the same experiment using Oregon Green 488 BAPTA-6F, which has a K_d of 3 μM ($n = 4$) and Oregon Green 488 BAPTA-5N ($n = 7$), which has a K_d of 20 μM. As shown in Fig. 2, local hot spots and a delayed spread through the terminal accompanying depolarizing steps of 200 ms or longer were visible even when using Oregon Green 488 BAPTA-5N, suggesting that intraterminal $[Ca^{2+}]$ attains micromolar concentrations. Similar results were also seen with Oregon Green 488 BAPTA-6F (data not shown; $n = 4$). With the low-affinity dyes, calcium changes were observed only in the synaptic regions even with depolarizing steps up to 1 s in duration (Fig. 3), consistent with the suggestion that calcium channels are concentrated in the terminal (Steele *et al*., 2005;Xu & Slaughter, 2005). With the high-affinity Oregon Green 488 BAPTA-1, small calcium increases were also observed in the cell bodies of both rods and cones in response to longer depolarizing steps.

We calculated the velocity of the delayed spread of calcium through rod terminals evoked by depolarizing steps of 0.5–1 s. To do so, we measured the distance traveled by a calcium wave to attain a defined fluorescence value as it spread through the terminal. The velocity of the calcium wave evoked by 0.5- and 1-s steps averaged 8.9 ± 0.8 and 8.3 ± 0.7 μm/s ($n = 32$), respectively. These values are similar to calcium wave velocities arising from CICR in other tissues (e.g. 10 μm/s, uterine myocytes, Young & Zhang, 2001; 6.6 μm/s, frog eggs, Bugrim *et al*., 2003); higher velocities can be attained at higher temperatures (Hennig *et al*., 2002). If one assumes that the waves result from diffusion, then these velocity values would yield diffusion coefficients of 34–40 $\mu m^2/s$, similar to the diffusion coefficients for calcium estimated in other preparations using a variety of techniques (10–65 $\mu m^2/s$: Kushmerick & Podolsky, 1969; Allbritton *et al*., 1992; Al-Baldawi & Abercrombie, 1995; Gabso *et al*., 1997; Nakatani *et al*., 2002) and many times slower than free diffusion in the absence of calcium buffering and sequestering mechanisms (140–300 $\mu m^2/s$: Allbritton *et al*., 1992; Al-Baldawi & Abercrombie, 1995).

We analysed the kinetics of intraterminal $[Ca^{2+}]$ changes by varying the duration of a depolarizing test pulse. For single-wavelength dyes such as Oregon Green, $\Delta F/F$ provides a measure of intracellular $[Ca^{2+}]$ independent of changes in dye concentration (Helmchen, 2000). We measured $\Delta F/F$ at hot spots in the terminals of rods, reasoning that these local hot spots probably correspond to clusters of calcium channels associated with individual ribbons (Nachman-Clewner *et al*., 1999; Zenisek *et al*., 2004). As shown in the graph in Fig. 4, $[Ca^{2+}]_i$ increased in rod terminals as the step duration was increased from 50 ms to 1 s. The abrupt increase in calcium levels measured at the hot spot when the step duration was increased from 100 to 200 ms was accompanied by a wave of calcium spreading through the terminal, whereas calcium changes evoked by shorter steps were restricted to local hot spots, as illustrated in Figs 2 and 3.

To test whether the secondary increase and wave of calcium through rod terminals evoked by longer test steps was due to CICR, we used a high concentration of ryanodine to block ryanodine receptors (Meissner, 1994). Consistent with CICR, the delayed spread of calcium through the

terminal was greatly diminished by introducing ryanodine (25 μM) directly into the cell through the patch pipette (Fig. 5). To quantify these effects, we measured the Δ*F*/*F* values at the local hot spot after waiting at least 4 min for ryanodine to diffuse into the terminal and plotted these against the step duration. As shown in Fig. 4 (open squares), the inclusion of ryanodine in the patch pipette solution blocked the secondary increase in calcium levels measured at the hot spot that was normally evoked by steps of 200 ms or longer. The ability of ryanodine to block the calcium wave and secondary increase in local calcium levels near the release site suggests they are both due to CICR. The ability of CICR to boost calcium levels near the release site during maintained depolarization is consistent with the possibility that CICR can regulate glutamate release from rod terminals.

Consistent with a significant contribution of CICR to synaptic transmission from rods, blocking CICR by bath application of ryanodine (25 μM) for at least 4 min reduced light-evoked currents in horizontal cells (Fig. 6A and B) by 72.6 ± 12.4% (n = 11) of control. Figure 6B amplifies and superimposes the same traces as in Fig. 6A to illustrate more clearly the effects of ryanodine on baseline and light-evoked currents. Light responses showed partial recovery to 54.1 ± 16.7% of control values after washout of ryanodine. Despite this partial recovery, ryanodine appeared to have persistent effects on retinal slices, as evidenced by the development of baseline current oscillations after washout. This is consistent with results from many preparations showing that it is difficult to reverse the effects of ryanodine following washout, but it is interesting to note that ryanodine has been reported to associate and dissociate from retinal membranes with higher rate constants than those found in cardiac and skeletal muscle (Shoshan-Barmatz *et al*., 2005). However, to avoid potential complications introduced by incomplete washout, we bath applied ryanodine only once on any retinal slice.

We tested whether the ryanodine-induced reduction in horizontal cell light responses might involve presynaptic effects by examining the actions of ryanodine on light-evoked voltage responses in rods. As shown in Fig. 6C, ryanodine (50 μM) diminished the peak light responses of rods evoked by a saturating flash by an average of 19.0 ± 11.1% (n = 7; P = 0.0039). Thus, some of the reduction in horizontal cell responses is due to an inhibition of rod light responses. However, the small reduction in rod light responses cannot explain the much greater reduction in horizontal cell light responses produced by ryanodine.

We also tested the effects of ryanodine on I_{Ca} measured in rods using a ramp voltage protocol. Consistent with results on L-type calcium channels in amacrine cells (Warrier *et al*., 2005), I_{Ca} was not altered by bath-applied ryanodine (50 μM, Fig. 6D, n = 5) or by ryanodine (50 μM) introduced directly into the cell through the patch pipette (data not shown, n = 4/4).

The results in Fig. 6 suggest that blocking CICR with ryanodine reduces synaptic transmission but the interpretation is complicated by the fact that ryanodine also reduces rod light responses. To avoid this complication, we circumvented the need for light stimulation by testing ryanodine (50 μM) on EPSCs evoked in horizontal cells by depolarizing steps applied directly to presynaptic rods. As illustrated in Fig. 7, 200-ms depolarizing steps from −70 to −10 mV applied to presynaptic rods evoked inward EPSCs in horizontal cells. The EPSC consisted typically of an initial fast transient inward current followed by a slower delayed inward current (Cadetti *et al*., 2005). Bath application of ryanodine (50 μM) had little effect on the initial transient component but reduced the later component of the EPSC. Similar effects of bath-applied ryanodine were obtained in 13/20 experiments with 50 μM ryanodine and 8/12 experiments with 25 μM ryanodine. Although, as mentioned previously, the persistence of baseline current oscillations suggested that complete recovery from ryanodine's effects was exceedingly slow, changes in the waveform of rod-evoked EPSC could sometimes be reversed by washout of ryanodine (Fig. 7A). Most of our studies were conducted on horizontal cells, but we also found that ryanodine (25–50 μM) inhibited later components of the PSC evoked

by depolarizing steps applied to rods in 5/5 OFF bipolar cells and 2/3 ON bipolar cells (data not shown).

To avoid potential postsynaptic effects of ryanodine on horizontal cells (Linn & Gafka, 2001; Solessio & Lasater, 2002; Huang *et al*., 2004), we also tested ryanodine by introducing it directly into the photoreceptor cell through the patch pipette. When comparing horizontal cell EPSCs evoked by depolarizing steps (−70 to −10 mV, 200 ms) applied to rods immediately after patch rupture with EPSCs evoked after ryanodine (50 μM) had diffused into the rod for 4–6 min, there was a pronounced reduction in later components of the EPSC, similar to results of bath-applied ryanodine (Fig. 7B). A similar reduction in later portions of the EPSC was observed in 10/14 experiments with 50 μM ryanodine and 2/4 experiments with 25 μM ryanodine. In control experiments in which ryanodine was omitted from the patch pipette solution, the EPSC consistently remained stable for periods much longer than 4–6 min after patch rupture, although it ultimately diminished due to response rundown (n = 14, Fig. 7C). Response rundown is accompanied by a preferential reduction in the early component of the EPSC (Fig. 7C, record at t = 45 min), in contrast with the reduction in later portions of the EPSC produced by including ryanodine in the pipette solution.

Ryanodine introduced through the patch pipette produced a similar inhibition of EPSCs evoked by steps to −30 mV (n = 6/8) as was observed with steps to −10 mV, suggesting a similar contribution of CICR at more depolarized membrane potentials.

Preferential inhibition of the later component of the EPSC by ryanodine suggests that this component arises from CICR. However, delayed components of the rod-evoked EPSC can also involve synaptic releases from neighboring rods stimulated by the spread of depolarizing current through gap junctions (Cadetti *et al*., 2005). We therefore tested whether inhibition of the PSC by ryanodine might involve inhibition of gap junctional coupling among rods. Consistent with its selectivity for CICR, ryanodine (50 μM) introduced through the patch pipette did not significantly alter the coupling conductance tested by applying voltage steps to one rod while recording simultaneously from a neighbouring rod (control: 494 ± 177 pS; ryanodine: 680 ± 435 pS; n = 4; P = 0.21, paired t-test).

Cone-driven EPSCs are consistently more transient than rod-driven EPSCs in both OFF bipolar and horizontal cells (Cadetti *et al*., 2005; Rabl *et al*., 2005). These rod/cone differences in EPSC kinetics are primarily due to differences in the rates of synaptic vesicle release by rods and cones (Cadetti *et al*., 2005). We tested whether the presence of CICR in rods might contribute to their slower synaptic release kinetics compared with cones. Release kinetics were assessed by measuring the charge transfer during EPSCs evoked by test pulses (−70 to −10 mV) of varying duration. Charge transfer was measured by integrating the area of the EPSC following baseline subtraction; charge transfer values were normalized to the charge transfer values measured for EPSCs evoked by 100-ms steps. CICR was blocked by introducing ryanodine (50 μM) into the presynaptic rod photoreceptor through the patch pipette; measurements were made > 4 min after patch rupture. Consistent with results from Rabl *et al*. (2005), plots of EPSC charge transfer vs. test step duration were fit by double exponential functions (Fig. 8). Time constants for the initial components were similar in ryanodine-treated (17.7 ms) and control cell pairs (19.8 ms). Consistent with imaging data indicating that CICR contributes significantly to intraterminal calcium increases evoked by steps longer than 100 ms (Fig. 4), introduction of ryanodine into the rod diminished the charge transfer accompanying EPSCs evoked by steps longer than 100 ms (Fig. 8). Charge transfer during EPSCs evoked by 200-ms depolarizing steps was reduced by 12.5% in ryanodine-treated cells compared with control cells (Fig. 8). This agreed with the 12.4% reduction in EPSCs evoked immediately after patch rupture compared with EPSCs evoked at least 4 min later after ryanodine had diffused into the rod (n = 9). Because the reduction in EPSC charge transfer measured in the

same cell before and after ryanodine did not have to be normalized, the agreement between these two measures suggests that the normalization procedure did not significantly distort the measurements shown in Fig. 8. Results in Fig. 8 support the hypothesis that CICR has a preferential impact on later components of release. The absence of significant differences in the initial component of release suggests that CICR is not a major contributor to the substantial rod/cone differences in the initial component of release and the faster resulting cone-driven EPSC waveform (Cadetti *et al*., 2005; Rabl *et al*., 2005).

Discussion

The present study provides evidence that CICR contributes to synaptic transmission from rods by showing that: (1) synaptic terminals are capable of CICR and (2) blocking CICR reduces post-synaptic responses at rod synapses. Evidence for these two conclusions are provided by the following observations. (1) Consistent with CICR in rod terminals, activation of ryanodine receptors by low concentrations of ryanodine stimulated calcium increases in the synaptic terminals and inner segments of rods in the retinal slice. These results support immunohistochemical studies suggesting the presence of ryanodine receptors on synaptic terminals and inner segments of isolated rods (Krizaj *et al*., 2003). Brief depolarizing steps applied to voltage-clamped rods stimulated local increases in calcium, presumably arising from influx through voltage-gated calcium channels. With longer test steps (≥ 200 ms), there was a secondary increase at the presumed site of influx accompanied by a wave of calcium spreading through the entire terminal. This secondary increase in calcium was inhibited by adding high concentrations of ryanodine to the patch pipette solution. These results suggest that CICR boosts intraterminal calcium levels in rods when depolarization is maintained for 200 ms or longer. (2) Blocking CICR with high concentrations of ryanodine inhibited EPSCs evoked in horizontal cells by depolarizing steps applied to presynaptic rods. Effects of ryanodine on the EPSC found in the present study are consistent with results of similar experiments by Suryanarayanan & Slaughter (2006). In support of the hypothesis that the secondary increase in intraterminal calcium levels evoked by depolarizing steps of 200 ms or longer provides a boost to synaptic transmission, high concentrations of ryanodine preferentially reduced later portions of the EPSCs in horizontal cells evoked by depolarizing steps maintained for 200 ms or longer.

In addition to inhibiting EPSCs evoked by depolarizing steps in paired recordings, high antagonist concentrations of ryanodine strongly inhibited light-evoked currents in horizontal cells. Part of the reduction in horizontal cell light-evoked responses is due to effects of ryanodine on presynaptic light-evoked voltage responses in rods (Fig. 6). Suryanarayanan & Slaughter (2006) observed no effect of ryanodine on rod light responses. Although ryanodine had no effect on the light response of one of the seven cells that we tested, we found that on average ryanodine inhibited rod light responses by 19%. Reasons for these differences in the two studies are unclear. The inhibitory effects of ryanodine found in our study recovered after washout, indicating that the inhibition was not simply response rundown (Fig. 6) and solvent control experiments showed no significant effect of the highly diluted ethanol used to dissolve ryanodine. Nonetheless, this 19% reduction in rod light responses cannot account for the 73% reduction in horizontal cell responses. Furthermore, the post-synaptic effect of reducing the peak hyperpolarizing voltage attained by rods in response to light is likely to be even less than 19% because of the diminishing amplitude of I_{Ca}, and therefore synaptic release, at more negative membrane potentials (Attwell *et al*., 1987;Witkovsky *et al*., 1997). Thus, much of the large reduction in horizontal cell light responses likely results from a reduction in synaptic output from photoreceptors.

Rods are relatively depolarized in darkness with resting membrane potentials of −40 to −45 mV. Suryanarayanan & Slaughter (2006) reported that ryanodine blocked EPSCs evoked by

mild depolarizing steps more effectively than it blocked EPSCs evoked by strong depolarizing steps, although we found little difference in the effects of ryanodine on EPSCs evoked by steps to −10 or −30 mV applied to rods. Our results suggest that the particularly potent effect of ryanodine on horizontal cell light responses compared with rod-driven EPSCs also involves the greater contribution of CICR to synaptic output when the membrane potential is maintained in a depolarized state for long periods of time (e.g. in darkness).

The contribution of CICR to release from tonically depolarized rod terminals is analogous to the contribution of CICR to spontaneous release at other synapses (Collin *et al*., 2005). The present results are also consistent with a role for CICR in synaptic release from the ribbon synapse in vestibular hair cells (Lelli *et al*., 2003). By contrast with its effects in vestibular hair cells, CICR in cochlear hair cells inhibits release by stimulating calcium-activated potassium channels that hyperpolarize the cell (Beurg *et al*., 2005). Effects of ryanodine on calcium-dependent ion currents in rods may also contribute to changes in synaptic output. The sensitivity of calcium-activated chloride channels in photoreceptors to caffeine suggests that they can be activated by CICR (Barnes & Hille, 1989). Because the chloride equilibrium potential in rods is positive to the dark resting potential, activation of these channels would be expected to depolarize rods and thus stimulate release, although this stimulatory effect is likely to be opposed by direct effects of chloride on calcium channels (Thoreson *et al*., 2002). Stimulation of calcium-activated potassium channels in rod terminals by CICR would also be expected to enhance release by directly enhancing I_{Ca} (Xu & Slaughter, 2005), but the presence of TEA in the pipette solution limited their contribution to our experiments.

As one component of our study, we examined whether the contribution of CICR to release from rods contributes to marked differences in the kinetics of rod- and cone-driven EPSCs. Cone-driven EPSCs are much more transient than rod-driven EPSCs in both OFF bipolar and horizontal cells. These rod/cone differences in EPSC kinetics are not due to rod/cone differences in kinetics of I_{Ca} or the presence of different post-synaptic glutamate receptors at rod and cone synapses but are primarily due to differences in the rates of vesicle release by rods and cones (Cadetti *et al*., 2005; Rabl *et al*., 2005). The 10-fold faster release kinetics of cones is manifested in a 10-fold faster initial rise in PSC charge transfer as a function of step duration. By contrast with the role for CICR in rods, Krizaj *et al*. (2003) suggested that CICR contributes little to regulating intracellular calcium levels in cones. We tested the hypothesis that by sustaining synaptic output from rods, CICR might slow rod-driven PSC waveforms. However, contrary to this hypothesis, a high concentration of ryanodine did not convert slow rod-driven PSCs into fast cone-driven PSCs nor did it produce faster cone-like release kinetics in the PSC charge transfer vs. duration plot.

In summary, the present study suggests that CICR increases intraterminal calcium levels in rods and that this calcium increase contributes to changes in synaptic release. The effects of CICR become increasingly evident with maintained depolarization, suggesting that CICR is likely to make a particularly prominent contribution to release from rods that are tonically depolarized in darkness.

Acknowledgements

This study was supported by NIH grant EY-10542, NIH Grant P20 RR16469 from the INBRE Program of the National Center for Research Resources, and a postdoctoral fellowship from Fight for Sight to L.C.

Abbreviations

CICR

calcium-induced calcium release

EPSC

	excitatory postsynaptic current
I_{Ca}	calcium current

References

Al-Baldawi NF, Abercrombie RF. Calcium diffusion coefficient in *Myxicola* axoplasm. Cell Calcium 1995;17:422–430. [PubMed: 8521456]

Allbritton NLT, Meyer &, Stryer L. Range of messenger action of calcium ion and inositol 1,4,5-trisphosphate. Science 1992;258:1812–1815. [PubMed: 1465619]

Attwell D, Borges S, Wu SM, Wilson M. Signal clipping by the rod output synapse. Nature 1987;328:522–524. [PubMed: 3039370]

Barnes S, Hille B. Ionic channels of the inner segment of tiger salamander cone photoreceptors. J Gen Physiol 1989;94:719–743. [PubMed: 2482325]

Beurg M, Hafidi A, Skinner LJ, Ruel J, Nouvian R, Henaff M, Puel JL, Aran JM, Dulon D. Ryanodine receptors and BK channels act as a presynaptic depressor of neurotransmission in cochlear inner hair cells. Eur J Neurosci 2005;22:1109–1119. [PubMed: 16176352]

Boulenger JP, Patel J, Marangos PJ. Effects of caffeine and theophylline on adenosine and benzodiazepine receptors in human brain. Neurosci Lett 1982;30:161–166. [PubMed: 6287366]

Bugrim A, Fontanilla R, Eutenier BB, Keizer J, Nuccitelli R. Sperm initiate a Ca^{2+} wave in frog eggs that is more similar to Ca^{2+} waves initiated by IP3 than by Ca^{2+} Biophys J 2003;84:1580–1590. [PubMed: 12609862]

Cadetti L, Tranchina D, Thoreson WB. A comparison of release kinetics and glutamate receptor properties in shaping rod-cone differences in EPSC kinetics in the salamander retina. J Physiol (Lond) 2005;569:773–788. [PubMed: 16223761]

Collin T, Marty A, Llano I. Presynaptic calcium stores and synaptic transmission. Curr Opin Neurobiol 2005;15:275–281. [PubMed: 15919193]

Crosson CE, Willis JA, Potter DE. Effect of the calcium antagonist, nifedipine, on ischemic retinal dysfunction. J Ocul Pharmacol 1990;6:293–299. [PubMed: 2097313]

Doonan F, Donovan M, Cotter TG. Activation of multiple pathways during photoreceptor apoptosis in the rd mouse. Invest Ophthalmol Vis Sci 2005;46:3530–3538. [PubMed: 16186330]

Edward DP, Lam TT, Shahinfar S, Li J, Tso MO. Amelioration of light-induced retinal degeneration by a calcium overload blocker Flunarizine. Arch Ophthalmol 1991;109:554–562. [PubMed: 2012559]

Fox DA, Poblenz AT, He L, Harris JB, Medrano CJ. Pharmacological strategies to block rod photoreceptor apoptosis caused by calcium overload: a mechanistic target-site approach to neuroprotection. Eur J Ophthalmol 2003;13:S44–S56. [PubMed: 12749677]

Gabso M, Neher M, Spira ME. Low mobility of the Ca^{2+} buffers in axons of cultured *Aplysia* neurons. Neuron 1997;18:473–481. [PubMed: 9115740]

Hayashida Y, Yagi T. On the interaction between voltage-gated conductances and Ca(2+) regulation mechanisms in retinal horizontal cells. J Neurophysiol 2002;87:172–182. [PubMed: 11784740]

Helmchen, F. Calibration of fluorescent calcium indicators. In: Yuste, R.; Lanni, F.; Konnerth, A., editors. Imaging Neurons: a Laboratory Manual. Cold Spring Harbor Laboratory Press; New York: 2000. p. 32.1-32.9.

Hemara-Wahanui A, Berjukow S, Hope CI, Dearden PK, Wu SB, Wilson-Wheeler J, Sharp DM, Lundon-Treweek P, Clover GM, Hoda JC, Striessnig J, Marksteiner R, Hering S, Maw MA. A CACNA1F mutation identified in an X-linked retinal disorder shifts the voltage dependence of Cav1.4 channel activation. Proc Natl Acad Sci USA 2005;102:7553–7558. [PubMed: 15897456]

Hennig GW, Smith CB, O'Shea DM, Smith TK. Patterns of intracellular and intercellular Ca^{2+} waves in the longitudinal muscle layer of the murine large intestine in vitro. J Physiol 2002;543:233–253. [PubMed: 12181295]

Huang SY, Liu Y, Liang PJ. Role of Ca^{2+} store in AMPA-triggered Ca^{2+} dynamics in retinal horizontal cells. Neuroreport 2004;15:2311–2315. [PubMed: 15640746]

Krizaj D, Bao JX, Schmitz Y, Witkovsky P, Copenhagen DR. Caffeine-sensitive calcium stores regulate synaptic transmission from retinal rod photoreceptors. J Neurosci 1999;19:7249–7261. [PubMed: 10460231]

Krizaj D, Lai FA, Copenhagen DR. Ryanodine stores and calcium regulation in the inner segments of salamander rods and cones. J Physiol (Lond) 2003;547:761–774. [PubMed: 12562925]

Krizaj D, Liu X, Copenhagen DR. Expression of calcium transporters in the retina of the tiger salamander (*Ambystoma tigrinum*). J Comp Neurol 2004;475:463–480. [PubMed: 15236230]

Kushmerick MJ, Podolsky RJ. Ionic mobility in muscle cells. Science 1969;166:1297–1298. [PubMed: 5350329]

Lelli A, Perin P, Martini M, Ciubotaru CD, Prigioni I, Valli P, Rossi ML, Mammano F. Presynaptic calcium stores modulate afferent release in vestibular hair cells. J Neurosci 2003;23:6894–6903. [PubMed: 12890784]

Linn CL, Gafka AC. Modulation of a voltage-gated calcium channel linked to activation of glutamate receptors and calcium-induced calcium release in the catfish retina. J Physiol 2001;535:47–63. [PubMed: 11507157]

Meissner G. Ryanodine receptor/Ca^{2+} release channels and their regulation by endogenous effectors. Annu Rev Physiol 1994;56:485–508. [PubMed: 7516645]

Mercurio AM, Holtzman E. Smooth endoplasmic reticulum and other agranular reticulum in frog retinal photoreceptors. J Neurocytol 1982;11:263–293. [PubMed: 6978386]

Nachman-Clewner M, St Jules R, Townes-Anderson E. L-type calcium channels in the photoreceptor ribbon synapse: localization and role in plasticity. J Comp Neurol 1999;415:1–16. [PubMed: 10540354]

Nakatani K, Chen C, Koutalos Y. Calcium diffusion coefficient in rod photoreceptor outer segments. Biophys J 2002;82:728–739. [PubMed: 11806915]

Pessah IN, Zimanyi I. Characterization of multiple [3H]ryanodine binding sites on the Ca^{2+} release channel of sarcoplasmic reticulum from skeletal and cardiac muscle: evidence for a sequential mechanism in ryanodine action. Mol Pharmacol 1991;39:679–689. [PubMed: 1851961]

Rabl K, Cadetti L, Thoreson WB. Kinetics of exocytosis is faster in cones than rods. J Neurosci 2005;25:4633–4640. [PubMed: 15872111]

Rousseau E, Smith JS, Meissner G. Ryanodine modifies conductance and gating behavior of single Ca^{2+} release channel. Am J Physiol 1987;253:C364–C368. [PubMed: 2443015]

Sharma AK, Rohrer B. Calcium-induced calpain mediates apoptosis via caspase-3 in a mouse photoreceptor cell line. J Biol Chem 2004;279:35564–35572. [PubMed: 15208318]

Shoshan-Barmatz V, Orr I, Martin C, Vardi N. Novel ryanodine-binding properties in mammalian retina. Int J Biochem Cell Biol 2005;37:1681–1695. [PubMed: 15896674]

Smith JB, Mills DC. Inhibition of adenosine 3′,5′-cyclic monophosphate phosphodiesterase. Biochem J 1970;120:20P.

Solessio E, Lasater EM. Calcium-induced calcium release and calcium buffering in retinal horizontal cells. Vis Neurosci 2002;19:713–725. [PubMed: 12688667]

Steele EC Jr, Chen X, Iuvone PM, MacLeish PR. Imaging of Ca^{2+} dynamics within the presynaptic terminals of salamander rod photoreceptors. J Neurophysiol 2005;94:4544–4553. [PubMed: 16107525]

Suryanarayanan A, Slaughter MM. Synaptic transmission mediated by internal calcium stores in rod photoreceptors. J Neurosci 2006;26:1759–1766. [PubMed: 16467524]

Thoreson WB, Nitzan R, Miller RF. Reducing extracellular chloride suppresses dihydropyridine-sensitive calcium currents and synaptic transmission in amphibian photoreceptors. J Neurophysiol 1997;77:2175–2190. [PubMed: 9114264]

Thoreson WB, Stella SL Jr, Bryson EJ, Clements J, Witkovsky P. D_2-like dopamine receptors promote interactions between calcium and chloride channels that diminish rod synaptic transfer in the salamander retina. Vis Neurosci 2002;19:235–247. [PubMed: 12392173]

Ungar F, Piscopo I, Holtzman E. Calcium accumulation in intracellular compartments of frog retinal rod photoreceptors. Brain Res 1981;205:200–206. [PubMed: 6970606]

Warrier A, Borges S, Dalcino D, Walters C, Wilson M. Calcium from internal stores triggers GABA release from retinal amacrine cells. J Neurophysiol 2005;94:4196–4208. [PubMed: 16293593]

Witkovsky P, Schmitz Y, Akopian A, Krizaj D, Tranchina D. Gain of rod to horizontal cell synaptic transfer: relation to glutamate release and a dihydropyridine-sensitive calcium current. J Neurosci 1997;17:7297–7306. [PubMed: 9295376]

Xu JW, Slaughter MM. Large-conductance calcium-activated potassium channels facilitate transmitter release in salamander rod synapse. J Neurosci 2005;25:7660–7668. [PubMed: 16107652]

Young RC, Zhang P. The mechanism of propagation of intracellular calcium waves in cultured human uterine myocytes. Am J Obstet Gynecol 2001;184:1228–1234. [PubMed: 11349193]

Zenisek D, Horst NK, Merrifield C, Sterling P, Matthews G. Visualizing synaptic ribbons in the living cell. J Neurosci 2004;24:9752–9759. [PubMed: 15525760]

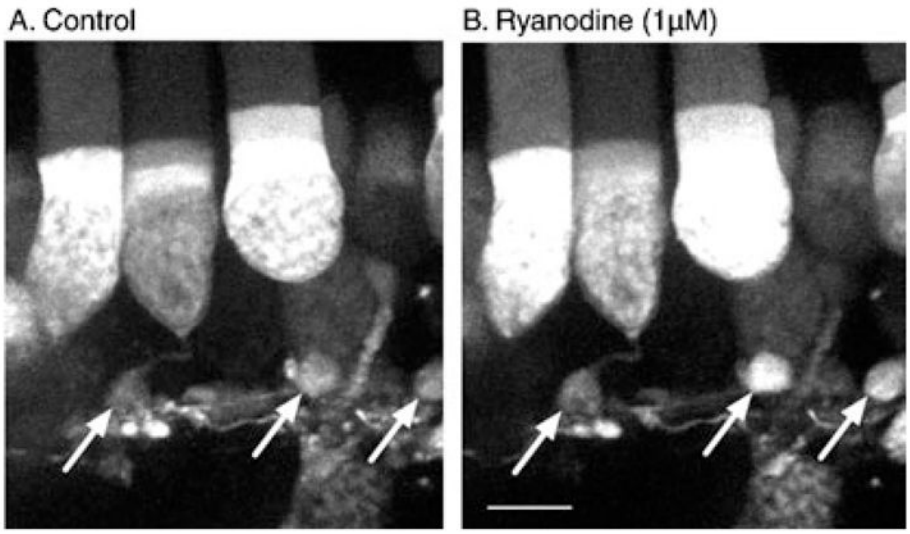

Fig. 1.

Bath-applied ryanodine (1 μM) stimulated Ca^{2+} increases in terminals and cell bodies of rods loaded with the calcium-sensitive dye Fluo4. (A) Control image. (B) Image obtained after bath application of ryanodine for 3 min. The images show stacks of confocal sections taken at 1-μm intervals. Image acquisition time was 125 ms per confocal slice. Rod terminals are indicated by arrows; readily detectable increases are visible in the two terminals at right; little increase was observed in the terminal at left. Ryanodine was bath applied for 3 min. Scale bar, 10 μm.

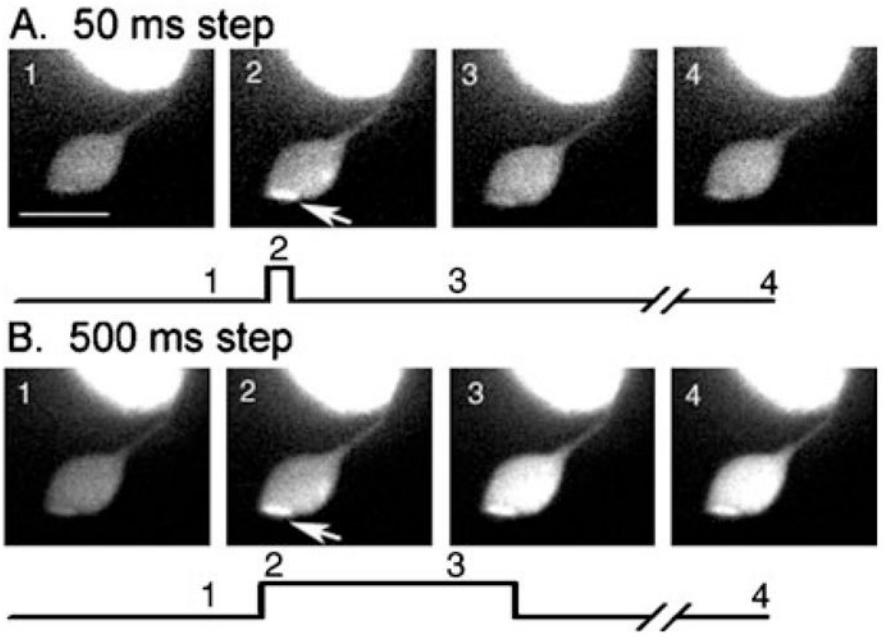

Fig. 2.

Changes in $[Ca^{2+}]_i$ in the synaptic terminal of a voltage-clamped rod in the retinal slice evoked by depolarizing steps (−70 to −10 mV). Calcium changes were visualized by including a high-affinity calcium-sensitive dye, Oregon Green 488 BAPTA-1 (100 μM; K_d = 0.17 μM), in the patch pipette solution. This single confocal section was cropped to show the terminal, axon and base of the cell body. The top row (A) shows responses to a step of 50 ms; the bottom row (B) shows responses to a step of 500 ms. Image timing is shown diagramatically below each set of images. Image 1 is a control image obtained prior to the step. Image 2 shows the image obtained at the beginning of the test step. For the 50-ms step (A), image 3 was obtained 250 ms after the end of the 50-ms test step whereas for the 500-ms step (B), image 3 was obtained 300 ms into the test step. Image 4 in A and B were both obtained 2.5 s after the beginning of the test step. Arrows point to a local hot spot of Ca^{2+} increase. Image acquisition time: 55 ms. Scale bar, 10 μm.

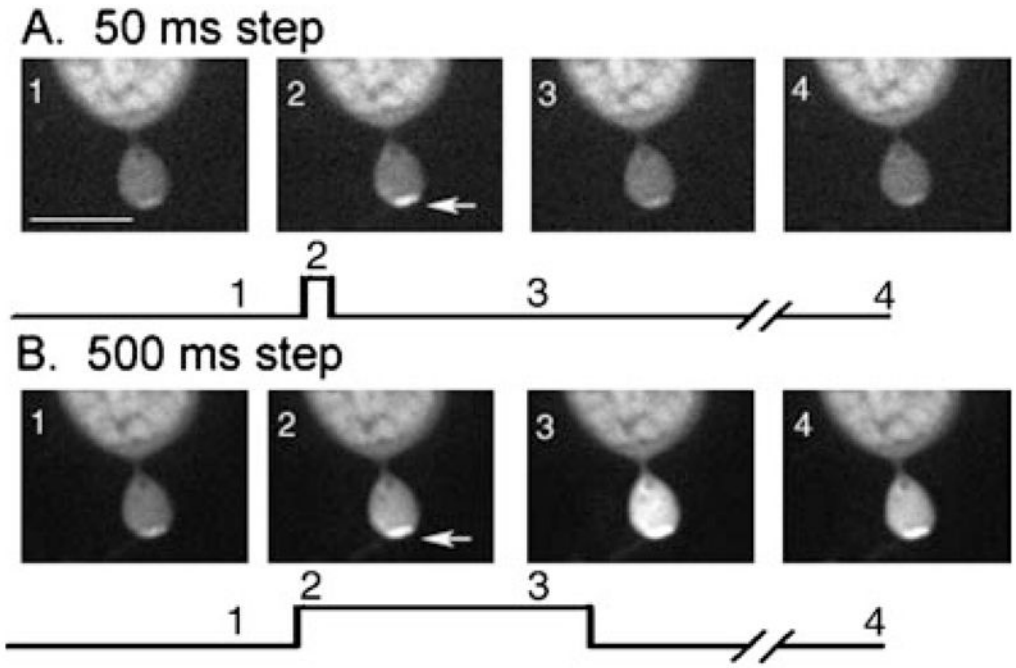

Fig. 3.

Changes in $[Ca^{2+}]_i$ in a single confocal slice from a rod terminal in the retinal slice evoked by depolarizing steps (−70 to −10 mV). Calcium changes were visualized by including a low-affinity calcium-sensitive dye, Oregon Green 488 BAPTA-5N (100 μM; K_d = 20 μM), in the patch pipette solution. The images show the terminal, axon and base of the cell soma. The top row (A) shows responses to a step of 50 ms; the bottom row (B) shows responses to a step of 500 ms. Image timing is shown diagramatically below each set of images. Image 1 shows a control image obtained prior to the step. Image 2 shows the image obtained at the beginning of the test step. For the 50-ms step (A), image 3 shows the image beginning 400 ms after termination of the 50-ms test step. For the 500-ms step (B), image 3 shows the last image obtained during the test step. Arrows indicate a local hot spot of Ca^{2+} increase. Image acquisition time: 48 ms. Scale bar, 10 μm.

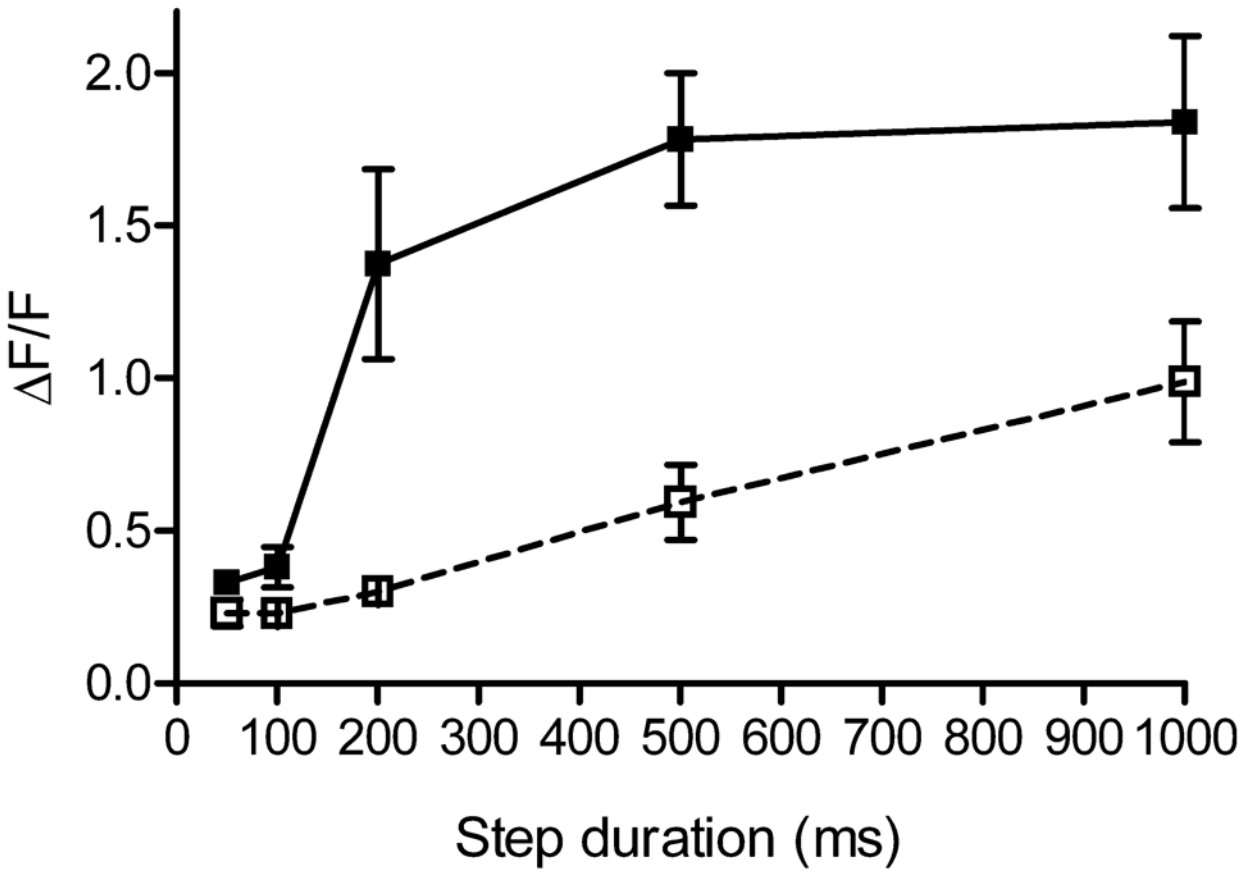

Fig. 4.

Intraterminal calcium levels increase with duration of the test step (−70 to −10 mV). Calcium levels (Δ*F*/*F*) were measured using the dye Oregon Green 488 BAPTA 5N at the hot spot in rod terminals. In control conditions, calcium levels (filled squares and solid line, $n = 7$) increased abruptly when the step was lengthened from 100 to 200 ms, accompanying the spread of calcium through the terminal illustrated in Figs 2 and 3. Introducing ryanodine (25 μM, open squares and dashed line, $n = 5$) into rods through the patch pipette abolished the abrupt increase in calcium levels measured at the hot spot, in addition to inhibiting the secondary spread evoked by longer steps as shown in Fig. 5.

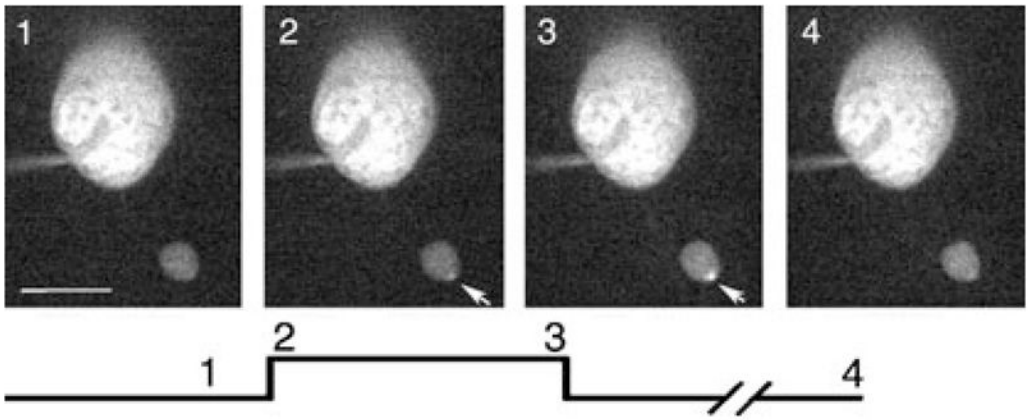

Fig. 5.

Addition of ryanodine (25 μM) to the pipette solution reduced the secondary spread of calcium through the rod terminal. Changes in $[Ca^{2+}]_i$ in a single confocal slice from a rod terminal in the retinal slice evoked by depolarizing steps (−70 to −10 mV, 500 ms). The images show the terminal and cell soma. Image timing is shown diagramatically below the images. Image 1 shows a control image obtained prior to the step. Image 2 shows the first image obtained during the test step. Image 3 shows the last image obtained during the 500-ms test step. Arrows indicate a local hot spot of Ca^{2+} increase. Pipette solution contained the low-affinity Ca^{2+} sensitive dye Oregon Green 488 BAPTA-5N (100 μM). Image acquisition time: 48 ms. Scale bar, 10 μm.

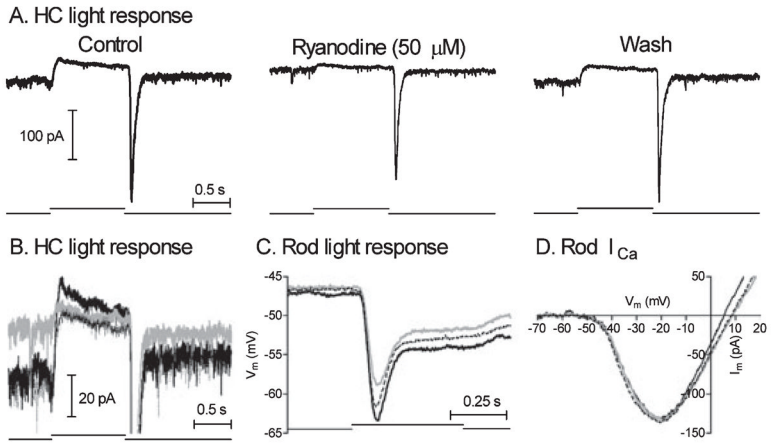

Fig. 6.

Bath-applied ryanodine (50 μM) strongly inhibited light-evoked currents in a horizontal cell (HC; panels A and B) but produced only a weak inhibition of light-evoked voltage responses in rods (C) and had no effect on rod I_{Ca} measured using a ramp voltage protocol (D). The three traces from A are superimposed in B to illustrate better ryanodine-induced changes in the waveform of the light-evoked current. For the records in panels B, C and D: solid black trace, control; grey trace, ryanodine; and thin dotted black trace, wash.

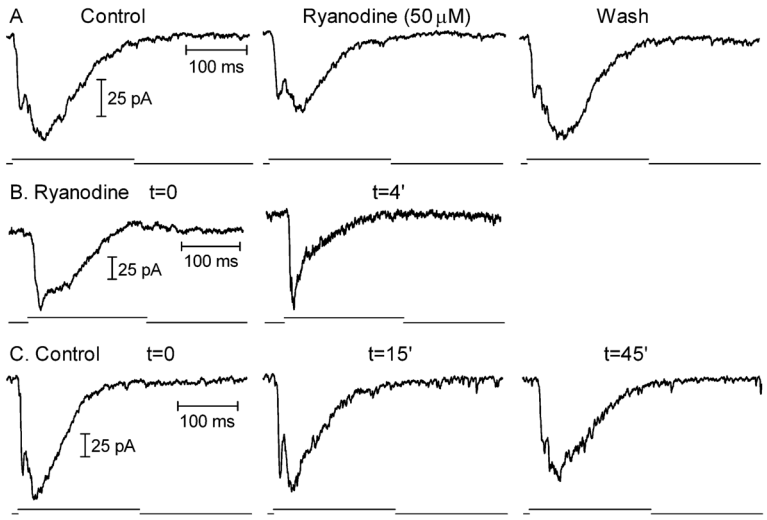

Fig. 7.

Blocking CICR with high concentrations of ryanodine inhibited EPSCs evoked in horizontal cells by depolarizing steps (−70 to −10 mV, 200 ms) applied to rods. (A) Bath-applied ryanodine (50 μM) inhibited a later component of the EPSC. The EPSC recovered following washout. (B) Introducing ryanodine (50 μM) directly into the rod through the patch pipette also reduced a later component of the EPSC. The control record was obtained immediately after rupturing into the rod and the ryanodine record was obtained 4 min later. (C) EPSCs remained stable for long periods in control recordings in which ryanodine was omitted from the pipette solution. The record on the left was obtained immediately after patch rupture and the records to the right were obtained 15 and 45 min later, respectively. As illustrated by the record obtained 45 min after patch rupture, response rundown was accompanied by a preferential reduction in the early, fast component of the EPSC, not the later portions that were preferentially reduced by ryanodine.

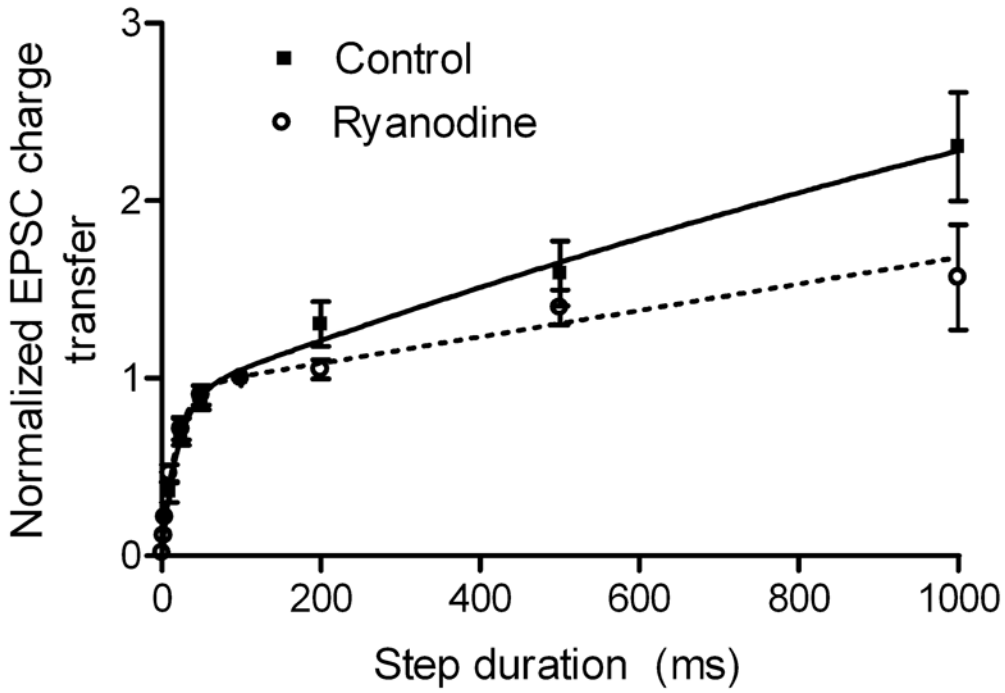

Fig. 8.

Intracellular ryanodine (50 μM) slightly reduced EPSC charge transfer for steps ≥ 200 ms, but did not significantly alter the initial component of release from rods. Data were fit with the bi-exponential function $A = Amp_1(1 - \exp(-t/\tau_1) + Amp_2(1 - \exp(-t/\tau_2)$ where A = amplitude of normalized EPSC charge transfer and t = step duration. Control (solid line): τ_1 = 19.8 ms, Amp_1 = 0.89, τ_2 = 2.6 s, Amp_2 = 4.3. Ryanodine (dashed line): τ_1 = 17.7 ms, Amp_1 = 0.93, τ_2 = 72.4 s, Amp_2 = 54.2. Control (filled squares): n = 10. Ryanodine (open circles): n = 7.